Hollow Fiber Reverse Osmosis Systems Analysis and Design

WILLIAM N. GILL

Faculty of Engineering
and Applied Sciences
State University of New York
Buffalo, New York 14214

and
BIHARI BANSAL

Chemical Engineering Department
Clarkson College of Technology
Potsdam, New York

A predictive model of hollow fiber reverse osmosis systems is developed using the equivalent annulus assumption. The fraction of feed recovered Φ depends on five parameters. Optimum values exist for the ratio of the inside to outside fiber radius r_i/r_o and for the outside fiber radius r_o. For dilute systems, a simple closed form expression is obtained for Φ which enables one to determine optimum values easily.

The effects of pressure, temperature, flow rate, concentration, viscosity of the feed, system length, membrane rejection parameter, and number of fibers are studied. Countercurrent is superior to concurrent operation.

SCOPE

The development of hollow fiber reverse osmosis systems has occurred within the last 5 years. There appears to be no predictive model available for determining the design and operational characteristics of these interesting membranes which are actually thick-walled cylinders that range from about 50 to 200 microns in outside diameter. The objectives of this study of hollow fiber units are to:

1. Develop a model of these systems from first principles for concurrent and countercurrent configurations;
2. Determine the relevant parameters which govern their behavior;
3. Demonstrate how the results can be used to describe the operating characteristics of such systems as a function of operating pressure, feed flow rate, temperature, and concentration;
4. Establish design criteria for wall thickness, outside radius, fiber length, and number of fibers;
5. Determine if the predicted results are consonant with available experimental and design data.

Previously reported work has dealt primarily with the general development of the fibers and their application to particular separations. The enormous surface area to volume ratio of hollow fiber systems makes them attractive for desalination, biological separations, waste water treatment, and a variety of other uses.

CONCLUSIONS AND SIGNIFICANCE

The distinguishing characteristic of hollow fiber systems is the enormous surface area they provide per unit volume. As a consequence concentration polarization is negligible, an appreciable pressure drop occurs along the system, and a large fraction of the feed can be removed in a single pass.

The geometry of hollow fiber systems is complicated; therefore, a simplified model is needed to make a mathematical analysis feasible. The equivalent annulus or free surface model is used in this work. Also, the use of a rejection coefficient R to characterize membrane selectivity is a major simplification which is reasonably satisfactory. Comparison of the theory with experimental data indicates that R varies only by about 2% over the range $0 \leq \Phi \leq 0.5$. However, the product concentration is sensitive even to small changes in R.

The present analysis shows that the membrane properties (A, R), the fluid properties (μ), the operating properties $(B_2, F, \Delta P)$, and the geometrical design properties $(l, N, r_i, r_o, \epsilon)$ can be combined into five dimensionless parameters which completely determine the behavior of both concurrent and countercurrent systems. Countercurrent flow is found to be superior to concurrent operation. In contrast to countercurrent flow, increasing the length of a concurrent system may reduce its productivity.

When the feed is dilute and the ratio of the osmotic pressure to hydrostatic pressure of the feed approaches zero, $B_2 \simeq 0$, the number of significant parameters is reduced from five to three and a closed form simple analytical expression for the fraction of feed recovered $\Phi(a, b, \xi_T)$ is obtained. For dilute solutions the difference between the feed pressure and the outlet pressure ΔP, the flow rate F, and the number of fibers N, arise in a single grouping $\Delta PN/F$, which appears only in the parameter a, which is of primary importance in determining system behavior. The analytical expression for $\Phi(a, b, \xi_T)$ in dilute systems is particularly useful in determining optimum values of the geometrical factors such as outside fiber radius r_o, inside fiber radius r_i, and fiber length l. Optimum values of these design variables depend on the operating conditions and can be determined by constraining the system to constant surface area and volume in which case one can fix only two of the four geometry variables l, N, r_o, and ϵ. As the length l of the system increases, the per-

formance becomes particularly sensitive to choosing the proper value of the outside fiber radius r_o, or void fraction ϵ.

Experimental operating data of Cooke (1969) and empirically determined values of the design variables are in good agreement with the theory.

In the last few years the development of hollow fiber membranes has attracted considerable attention for various reverse osmosis applications. These heavy-walled, hollow cylindrical membranes are spun from semipermeable polymeric material. The cylinders are called fibers because of their extremely small diameter which ranges from 50 to 200 microns.

Usually, the U-shaped fibers are potted in an epoxy resin tube sheet and are housed in a shell. Pressurized feed solution flows over the fibers in the shell. The product water permeates the fibers and flows inside them toward the open ends which are exposed to atmospheric pressure. This arrangement can be either concurrent or countercurrent.

The primary advantages of hollow fibers are that they provide large membrane area per unit volume and they are strong enough not to require the use of a support tube. To increase the area to volume ratio, it is desirable to use fibers with the smallest outside radius. However, it will be shown in the present work that given the overall surface area of the fibers and shell volume, there is an optimum fiber radius which maximizes system productivity.

To date, very little work on hollow fibers has been reported in the literature (Cooke, 1969; Mahon, 1966; and Orofino, 1970). However, a considerable body of literature does exist which deals with conventional reverse osmosis systems, and this has been recently summarized by Gill et al. (1971).

Reverse osmosis in hollow fibers differs from larger diameter membranes in several ways:

1. Concentration polarization in hollow fibers is negligible because of the large surface area and small product flux.
2. Pressure varies axially due to large friction losses and product removal.
3. Up to 80% of feed is removed so concentration builds up significantly.
4. Solution and product sides of hollow fibers are coupled.
5. Hollow fiber geometry is complicated.

MATHEMATICAL FORMULATION

It is assumed that the fibers are arranged on an equilateral triangular pitch. Because variations in concentration and pressure are small around the periphery of the hexagonal boundary surrounding each fiber, this boundary is replaced by an equivalent circular one having the same area in the annulus between it and the outside fiber wall. This approximation is the equivalent annulus or free surface model which has been used successfully by Happel (1959), by Sparrow and Loeffler (1959), and by Sparrow et al. (1961) in solving related problems.

Figure 1 shows a typical fiber; the positive z direction is from left to right and the positive radial direction is outward. The outside fiber radius r_o and the equivalent radius r_e are related by

$$r_e = \left(\frac{1}{1-\epsilon}\right)^{1/2} r_o$$

where ϵ is the porosity or void fraction of the fiber bundle.

Feed solution is in phase (1); the solid fiber is phase (2); and the product side is phase (3). It is assumed that steady laminar flow exists in the system; the fluid is Newtonian and has constant physical properties; the angular component of the velocity is zero and the system has peripheral symmetry. The last assumption follows from the free surface approximation. Axial mass diffusion and free convection effects are neglected and the temperature is assumed constant. The assumption of constant temperature is conservative.

Governing Differential Equations and Boundary Conditions

The equations for conservation of momentum and mass, then, take the following form:

$$u_i \frac{\partial u_i}{\partial z} + v_i \frac{\partial u_i}{\partial r} = -\frac{1}{\rho}\frac{\partial p_i}{\partial z} + \nu\left[\frac{\partial^2 u_i}{\partial z^2} + \frac{1}{r}\frac{\partial}{\partial r} r \frac{\partial u_i}{\partial r}\right] \quad (1)$$

$$u_i \frac{\partial v_i}{\partial z} + v_i \frac{\partial v_i}{\partial r} = -\frac{1}{\rho}\frac{\partial p_i}{\partial r} + \nu\left[\frac{\partial^2 v_i}{\partial z^2} + \frac{\partial}{\partial r}\frac{1}{r}\frac{\partial}{\partial r}(r v_i)\right] \quad (2)$$

$$\frac{\partial u_i}{\partial z} + \frac{1}{r}\frac{\partial}{\partial r}(r v_i) = 0 \quad (3)$$

$$u_i \frac{\partial c_i}{\partial z} + v_i \frac{\partial c_i}{\partial r} = D \frac{1}{r}\frac{\partial}{\partial r} r \frac{\partial c_i}{\partial r} \qquad i = 1, 2, 3 \quad (4)$$

The boundary conditions are as follows:

Phase (1)

$$u_1(0, r) = u_{1m}(0) h(r) \quad \text{(fully developed inlet velocity profile)} \quad (5a)$$

$$u_1(z, r_o) = 0 \quad \text{(no slip)} \quad (5b)$$

$$v_1(z, r_o) = v_{1w}(z) \quad \text{(unknown permeation velocity to be determined)} \quad (5c)$$

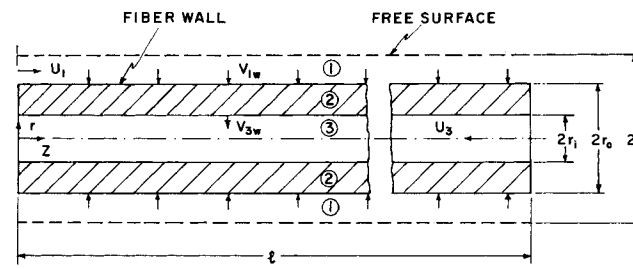

Fig. 1. Coordinate system for a fiber in countercurrent flow.

$$\frac{\partial u_1}{\partial r}(z, r_e) = 0 \qquad \text{(no shear at } r = r_e) \qquad (5d)$$

$$v_1(z, r_e) = 0 \qquad \text{(no material flow across } r = r_e) \qquad (5e)$$

$$c_1(0, r) = c_o \qquad \text{(uniform inlet feed concentration)} \qquad (6a)$$

$$\frac{\partial c_1}{\partial r}(z, r_e) = 0 \qquad \text{(symmetry at } r = r_e) \qquad (6b)$$

$$D\frac{\partial c_1}{\partial r}(z, r_o) = Rv_{1w}(z)c_1(z, r_o) \qquad \text{(continuity of salt flux)} \qquad (6c)$$

Phase (2)

$$v_2(z, r_o) = v_{1w}(z) \qquad \text{(unknown permeation velocity)} \qquad (7a)$$

$$u_2(z, r) = 0 \quad r_i \leq r \leq r_o, \quad 0 \leq z \leq l \qquad \text{(no axial flow in fiber wall)} \qquad (7b)$$

Phase (3)

$$\left.\begin{aligned} u_3(l, r) &= 0 \qquad \text{(countercurrent flow)} \\ u_3(0, r) &= 0 \qquad \text{(concurrent flow)} \end{aligned}\right\} \qquad (8a)$$

$$u_3(z, r_i) = 0 \qquad \text{(no slip)} \qquad (8b)$$

$$v_3(z, r_i) = \frac{r_o}{r_i} v_{1w}(z) \qquad \text{(unknown permeation velocity)} \qquad (8c)$$

$$\frac{\partial u_3}{\partial r}(z, 0) = 0 \qquad \text{(symmetry at fiber axis)} \qquad (8d)$$

$$v_3(z, 0) = 0 \qquad (8e)$$

The concentration c_2, in phase 2, is not needed since R, the rejection coefficient, is defined by

$$c_{3w} \equiv c_3(z, r_i) = (1 - R)c_{1w} = (1 - R)\, c_1(z, r_o) \qquad (9)$$

and R is assumed to be an intrinsic property of the membrane. The inlet velocity distribution on the shell side is given by

$$h(r) = \alpha_1 \left[\frac{r_e^2}{2r_o^2} \ln \frac{r}{r_o} - \frac{1}{4r_o^2}(r^2 - r_o^2) \right] \qquad (10)$$

where α_1 is defined as

$$\alpha_1 = \frac{r_e^2 - r_o^2}{\frac{r_e^4}{2r_o^2} \ln \frac{r_e}{r_o} - \frac{3}{8}\frac{r_e^4}{r_o^2} + \frac{r_e^2}{2} - \frac{r_o^2}{8}} \qquad (10a)$$

Note that it is not necessary to solve Equation (4) for phase (3) since the product concentration coming out at the fiber end exposed to the atmosphere can be calculated if c_{3w} and v_{1w} are known.

The wall velocity v_{1w} can be represented by

$$v_{1w} = -A[p_{1w} - p_{3w} - (\pi_{1w} - \pi_{3w})] \qquad (11)$$

Assuming a linear relationship between the concentration and the osmotic pressure and using the definition of R from Equation (9), Equation (11) becomes

$$v_{1w}(z) = -A\left[p_{1w} - p_{3w} - \frac{\pi_o}{c_o} R\, c_{1w}\right] \qquad (11a)$$

To compute v_{1w}, which is of prime interest, one needs to compute p_{1w}, p_{3w}, and c_{1w}.

Calculation of p_{1w}. Since l/r_o is on the order 10^4 and the Reynolds number in the shell is on the order unity, only fully developed regions are important. For constant wall velocity one can solve Equations (1) to (3) by using Berman's (1953) approach. Here the solution of Equations (1) to (3) is developed for variable wall velocity by using a perturbation method which is valid because $Re_w \approx 10^{-4}$. Since the flow is incompressible and two dimensional, we define a stream function as

$$u_1 = -\frac{1}{r}\frac{\partial \psi_1}{\partial r} \qquad (12)$$

$$v_1 = \frac{1}{r}\frac{\partial \psi_1}{\partial z} \qquad (13)$$

The boundary conditions and differential equations suggest the following form for the stream function:

$$\psi_1 = \left\{ u_{1m}(0)r_o + \frac{2r_o^2}{r_e^2 - r_o^2} \int_0^z v_{1w}(z)\, dz \right\} f_1(r, z) = r_o\, u_{1m}(z)\, f_1(r, z) \qquad (14)$$

where f_1 is an unknown function of z and r. The pressure is elminated from Equations (1) and (2) by cross-differentiation and equating mixed derivatives of pressure. Then, by using Equations (12) through (14), u_1 and v_1 can be expressed in terms of $u_{1m}(z)$ and f_1 and these results are inserted into the result of combining Equations (1) and (2). If one assumes that f_1 is a weak function of z so that derivatives with respect to z can be neglected, a fourth-order total differential equation for f_1 is obtained. The solution for f_1 can be obtained by using a perturbation expansion in the wall Reynolds number as

$$f_1(r) = f_{10}(r) + f_{11}(r)\, Re_w + f_{12}(r)\, Re_w^2 + \cdots \qquad (15)$$

By using Equation (15) and the total differential equation for f_1, one gets, for f_{10}, the following differential equation and the boundary conditions

$$\left[\frac{1}{r}\left\{ r\left(\frac{f'_{10}}{r}\right)' \right\}'\right]' = 0 \qquad (16)$$

$$\left.\begin{aligned} f'_{10}(r_o) &= f_{10}(r_e) = 0 \\ f_{10}(r_o) &= \frac{r_e^2 - r_o^2}{2r_o} \\ r_e f''_{10}(r_e) &= f'_{10}(r_e) \end{aligned}\right\} \qquad (16a)$$

which yields

$$f_{10} = \alpha_1 \left[\frac{r^4}{16r_o^3} - \frac{r^2}{8r_o} - \frac{r_e^2}{2r_o^2}\left\{ \frac{r^2}{2r_o} \ln \frac{r}{r_o} - \frac{r^2}{4r_o} \right\} + \alpha_2 \right] \qquad (17)$$

where

$$\alpha_2 = \frac{r_e^4}{4r_o^3} \ln \frac{r_e}{r_o} - \frac{3r_e^4}{16r_o^3} + \frac{r_e^2}{8r_o} \qquad (18)$$

With this result and Equations (1), (2), (12) (13), and (14) one gets

$$u_1(r, z) = \alpha_1\, u_{1m}(z) \left\{ \frac{r_e^2}{2r_o^2} \ln \frac{r}{r_o} - \frac{1}{4r_o^2}(r^2 - r_o^2) \right\} \qquad (19)$$

$$v_1(r, z) = \frac{2r_o^2\alpha_1}{r_e^2 - r_o^2} v_{1w}(z) \left[\frac{r^3}{16r_o^3} - \frac{r}{8r_o} - \frac{r_e^2}{2r_o^2}\left\{ \frac{r}{2r_o} \ln \frac{r}{r_o} - \frac{r}{4r_o} \right\} + \frac{\alpha_2}{r} \right] \qquad (20)$$

$$\frac{\partial p_1}{\partial z} = -\frac{\mu\alpha_1}{r_o^2} u_{1m}(z) + 0(Re_w) \tag{21}$$

$$\frac{\partial p_1}{\partial r} \stackrel{\wedge}{=} 0(Re_w) \tag{22}$$

and

$$u_{1m}(z) = u_{1m}(0) + \frac{2r_o}{r_e^2 - r_o^2} \int_0^z v_{1w}(z)\, dz \tag{23}$$

Equations (19) through (23) apply to both concurrent and countercurrent flows.

Calculation of p_{3w}: For flow inside the fiber,

$$\psi_3 = \left[\int_l^z v_{1w}(z)dz \right] f_3(r, z) \quad \text{countercurrent} \tag{24}$$

$$\psi_3 = \left[\int_0^z v_{1w}(z)dz \right] f_3(r, z) \quad \text{concurrent} \tag{25}$$

which yield the following expressions for the velocity and pressure fields inside the fiber.

$$u_3(z, r) = \begin{cases} -\dfrac{4r_o}{r_i^4}(r_i^2 - r^2) \displaystyle\int_l^z v_{1w}(z)dz & \text{countercurrent} \\ \dfrac{4r_o}{r_i^4}(r_i^2 - r^2) \displaystyle\int_0^z v_{1w}(z)dz & \text{concurrent} \end{cases} \tag{26}$$

$$v_3(z, r) = v_{1w}(z) \left[\frac{2r_o r}{r_i^2} - \frac{r_o r^3}{r_i^4} \right] \quad \text{Both countercurrent and concurrent} \tag{27}$$

$$\frac{dp_3}{dz} = \frac{-8\mu}{r_i^2} u_{3m}(z) \quad \text{Both countercurrent and concurrent} \tag{28}$$

where

$$u_{3m}(z) = \begin{cases} \dfrac{r_e^2 - r_o^2}{r_i^2}[u_{1m}(z) - u_{1m}(l)] & \text{countercurrent} \\ \dfrac{r_e^2 - r_o^2}{r_i^2}[u_{1m}(0) - u_{1m}(z)] & \text{concurrent} \end{cases} \tag{29}$$

Calculation of c_{1w}: Equation (4) for $i = 1$ will be solved after it is shown that concentration polarization is negligible. Since concentration polarization increases as v_{1w} increases and v_{1w} is a maximum at $z = 0$ (the driving force is greatest there), Equation (4) is solved for $i = 1$ and boundary conditions (6) under the most severe conditions which are

1. $v_{1w} = v_{1w}(0)$
2. large values of z

The first condition makes Equation (6c) a linear boundary condition so that the problem can be solved by using an orthogonal series expansion technique to give for large distances from the inlet,

$$\frac{c_{1w}}{c_{1b}} = \frac{\displaystyle\int_{r_o}^{r_e} r\, u_1(0, r)\, dr}{\displaystyle\int_{r_o}^{r_e} u_1(0, r)\, r \exp\left(\frac{1}{D} \int_{r_o}^{r} v_1(r')dr' \right) dr} \tag{30}$$

where c_{1b} is the bulk concentration in phase (1). Numerical results indicate that for all practical values of Pe_w, say $Pe_w \leq 10^{-1}$, concentration polarization is negligible. That is,

$$\frac{c_{1w}}{c_{1b}} \cong 1.0 \tag{31}$$

and therefore c_1 is essentially independent of r. Integrating Equation (4) (for $i = 1$) with respect to r from $r = r_o$ to $r = r_e$ and solving the resulting ordinary differential equation, one obtains

$$\frac{c_1}{c_o} = \frac{c_{1w}}{c_o} = \left[\frac{u_{1m}(0)}{u_{1m}(z)} \right]^R \tag{32}$$

This simple equation is valid for both concurrent and countercurrent flows.

General Equation for Countercurrent Flow

Now define the following dimensionless quantities:

$$\xi = \left[\frac{2A\mu\alpha_1 r_o}{r_e^2 - r_o^2} + \frac{16A\mu r_o^3}{r_i^4} \right]^{1/2} \frac{z}{r_o} \tag{33a}$$

$$a = \frac{\dfrac{2A\Delta P\, r_o^2}{u_{1m}(0)(r_e^2 - r_o^2)}}{\left[\dfrac{A\mu\alpha_1 r_o}{r_e^2 - r_o^2} + \dfrac{16A\mu r_o^3}{r_i^4} \right]^{1/2}} \tag{33b}$$

$$b = \frac{1}{1 + \dfrac{\alpha_1 r_i^4}{8r_o^2(r_e^2 - r_o^2)}} \tag{33c}$$

$$U_{1m} = \frac{u_{1m}(z)}{u_{1m}(0)} \tag{33d}$$

$$B_2 = \pi_o/\Delta P \tag{33e}$$

Substituting Equation (32) into Equation (11a), differentiating the resulting equation with respect to z, and using Equations (21), (23), (28), and (29), one gets

$$\frac{d^2U_{1m}}{d\xi^2} + \frac{a\, B_2 R^2}{U_{1m}^{R+1}} \frac{dU_{1m}}{d\xi} - U_{1m} = b(\Phi - 1) \tag{34}$$

where Φ, the fraction of feed recovered, has been defined by $\Phi \equiv [u_{1m}(0) - u_{1m}(l)]/u_{1m}(0)$. The appropriate boundary conditions are

$$U_{1m}(0) = 1 \tag{35a}$$

$$\frac{dU_{1m}}{d\xi}(0) = -a(1 - B_2 R) \tag{35b}$$

The last boundary condition is readily derived from Equations (11a) and (23).

General Equation for Concurrent Flow

Substituting Equation (32) into Equation (11a), differentiating the resulting equation with respect to z, and using Equations (21), (23), (28), and (29), one gets

$$\frac{d^2U_{1m}}{d\xi^2} + \frac{a\, B_2 R^2}{U_{1m}^{R+1}} \frac{dU_{1m}}{d\xi} - U_{1m} = -b \tag{36}$$

$$U_{1m}(0) = 1 \tag{37a}$$

$$\frac{dU_{1m}}{d\xi}(0) = -a\left[1 - \frac{p_3(0)}{\Delta P} - B_2 R \right] \tag{37b}$$

The last boundary condition is readily derived from Equa-

tions (11a) and (23). $p_3(0)$ is the pressure inside the fiber at $z = 0$.

Physical Meaning of Parameters

Clearly, Φ is a function of five parameters in general and this dependence can be expressed as

$$\Phi = 1 - U_{1m}(\xi_T) = \Phi[\xi_T, a, b, B_2, R]$$

where ξ_T stands for the total dimensionless length of the system. Now it is important to relate the model parameters to the physical parameters of hollow fiber systems. The void fraction ϵ of the bundle is given by

$$\epsilon = \frac{r_e^2 - r_o^2}{r_e^2} = 1 - \frac{r_o S}{2V} \tag{38a}$$

where S, the total surface area of all fibers, and V, the total volume of the system, are given by

$$S = 2\pi r_o N l \tag{38b}$$

$$V = \frac{\pi r_o^2 N l}{1 - \epsilon} \tag{38c}$$

Note that

$$u_{1m}(0) = \left(\frac{F}{\pi N}\right) \frac{1}{(r_e^2 - r_o^2)} \tag{38d}$$

and one can write a, b, and ξ_T in more useful form as

$$a = \left(\frac{A\mu}{r_o}\right)^{1/2} \left(\frac{2A\Delta P N r_o^3}{F\mu}\right) a_2^2 \left[a_2^4 g(\epsilon) + 16\right]^{-1/2} \tag{38e}$$

$$b = 16/\left[a_2^4 g(\epsilon) + 16\right] \tag{38f}$$

$$\xi_T = \left(\frac{A\mu}{r_o}\right)^{1/2} a_2^{-2} \left[a_2^4 g(\epsilon) + 16\right]^{1/2} \frac{l}{r_o} \tag{38g}$$

where a_2 and $g(\epsilon)$ have been defined in the Notation. Thus, it is possible to determine how the membrane properties (A, R), the fluid properties (μ), the operating properties (B_2, F, ΔP) and the geometric design properties (a_2, l, N, r_o, ϵ) affect the behavior of hollow fiber reverse osmosis systems. Also note that once the surface area S and volume V are fixed, only two of the four parameters (l, N, r_o, and ϵ) are independent.

Calculation of Product Concentration

Other than Φ, the fraction of feed recovered, the most important quantity is the product concentration at the outlet. To calculate this, first integrate Equation (3) with respect to r to get

$$v_{1w} = \frac{r_o \epsilon}{2(1 - \epsilon)} \frac{d u_{1m}}{dz} \tag{39}$$

From Equations (9) and (32) one has

$$c_{3w} = (1 - R)c_{1w} = (1 - R)c_o \left[\frac{u_{1m}(0)}{u_{1m}(z)}\right]^R \tag{40}$$

and a material balance on a differential axial element inside the fiber gives

$$d(u_{3m}c_{3b}) = \left[\frac{\epsilon(1 - R)c_o u_{1m}{}^R(0)}{a_2^2(1 - \epsilon)}\right] \frac{du_{1m}}{u_{1m}{}^R} \tag{41}$$

Integration of Equation (41) yields

$$\frac{c_p}{c_o} = \frac{1 - (1 - \Phi)^{1-R}}{\Phi} \tag{42}$$

Equation (42) can be rearranged to give

$$R = 1 - \frac{\ln\left[1 - \frac{c_p}{c_o}\Phi\right]}{\ln[1 - \Phi]} \quad \text{where } c_p = c_{3b}(0) \tag{43}$$

Equations (34) to (37) and Equation (42) govern the productivity and product concentration for hollow fiber countercurrent and concurrent flow arrangements.

Solutions for Dilute Systems, $B_2 = 0$

Countercurrent flow. Since the nonlinear term vanishes when $B_2 = 0$, Equation (34), subject to boundary conditions (35), is solved analytically and the expression for Φ is

$$\Phi = \frac{(1 - b) + a \sinh \xi_T - (1 - b) \cosh \xi_T}{1 - b + b \cosh \xi_T} \tag{44}$$

Concurrent flow. From Equations (36) and (37), the fraction of feed recovered is found to be

$$\Phi = \frac{a \sinh \xi_T + (1 - b)(1 - 2b)(1 - \cosh \xi_T) - b(1 - b)\xi_T \sinh \xi_T}{1 - b + b \cosh \xi_T} \tag{45}$$

Solutions for Concentrated Systems, $B_2 \neq 0$

Analytical solutions could not be found for the nonlinear equations (34) and (36), and it was necessary to solve them numerically. A fourth-order Runge-Kutta scheme was used together with a simple iterative procedure that converged rapidly. For the countercurrent system, a value of Φ was assumed and the forward solution was started. When either $v_{1w} = 0$ or $c_{3w} = c_o$ occurred, the integration was terminated. Beyond the axial location at which $c_{3w} = c_o$, it is apparent that no further benefit is derived by additional system length. Φ obtained as a result of the integration was compared with Φ assumed. If the two values did not agree, a new Φ was taken as

$$\Phi_{\text{new}} = \frac{[\Phi_{\text{old}} + \Phi_{\text{cal}}]}{2}$$

and the procedure was repeated.

RESULTS AND DISCUSSION

Maximum Possible Useful System Length, $B_2 = 0$

The maximum useful length is limited by either of the following two restrictions*:

1. The wall velocity becomes zero at some length beyond which the system is unproductive.
2. The entire feed is removed as product at which point $U_{1m} = 0$.

The dimensionless length at which either of these possibilities occurs is the maximum useful length $\xi_{\max}$. Simple expressions for $\xi_{\max}$ can be obtained for the special case of $B_2 = 0$.

For countercurrent flow the condition for the wall velocity to vanish is that a be less than unity and for $B_2 = 0$, $\xi_{\max}$ is

$$\xi_{\max} = \sinh^{-1}\left\{\frac{\sqrt{a(b + (1 - b)^2 - a^2(1 - 2b))}}{(1 - a^2)(1 - b)}\right\}, \quad v_{1w} \to 0 \tag{46}$$

* This assumes no solute precipitation.

The condition for the axial velocity U_{1m} to vanish is that a be greater than unity so that

$$\xi_{max} = \coth^{-1} a, \quad U_{1m} \to 0 \tag{47}$$

For concurrent flow, v_{1w} vanishes when

$$a = b(1-b)\,\xi_{max} + (1-b)^2 \tanh \xi_{max}, \quad v_{1w} \to 0 \tag{48}$$

Here, a depends on b and ξ_{max}. Similarly, the necessary condition for the axial velocity to vanish is

$$a = [(1-b)^2 + b^2] \coth \xi_{max} + \frac{2b(1-b)}{\sinh \xi_{max}} + b(1-b)\xi_{max}, \quad U_{1m} \to 0 \tag{49}$$

In concurrent systems, both the asymptotic value of Φ and the length required to recover a desired fraction of feed as product are influenced considerably by b. Under certain conditions, depending on a and b, Φ exhibits a maximum with increasing ξ_T. Therefore, one does not necessarily increase Φ by increasing the length; clearly, increasing ξ_T beyond the maximum is undesirable. The reason for this may be adduced readily. In concurrent systems when one increases the length, the surface area increases as does the pressure drop over the length l. Furthermore, in concurrent systems the entire product flows along the increased length and $p_3(0)$ must increase and this decreases the wall velocity. Thus, Φ may go through a maximum with increasing ξ_T. By contrast, in countercurrent systems when one increases the length, only the additional fluid retained in phase (3) flows through the entire length and compared to increasing the surface area for recovery, this effect is small. Therefore, Φ does not go through a maximum in countercurrent systems.

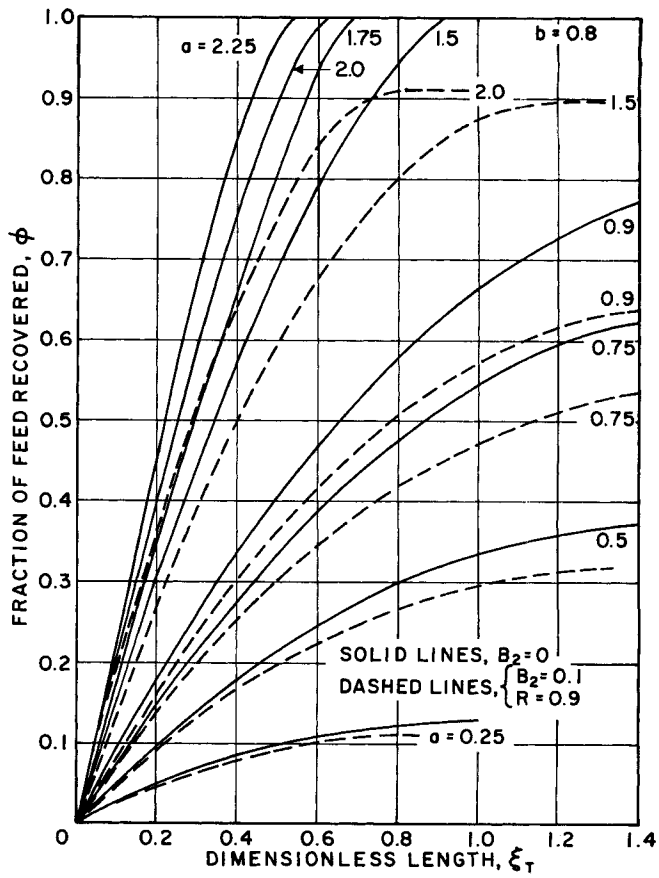

Fig. 3. Fraction of feed removed Φ vs. dimensionless length parameter ξ_T for countercurrent flow, $b = 0.8$.

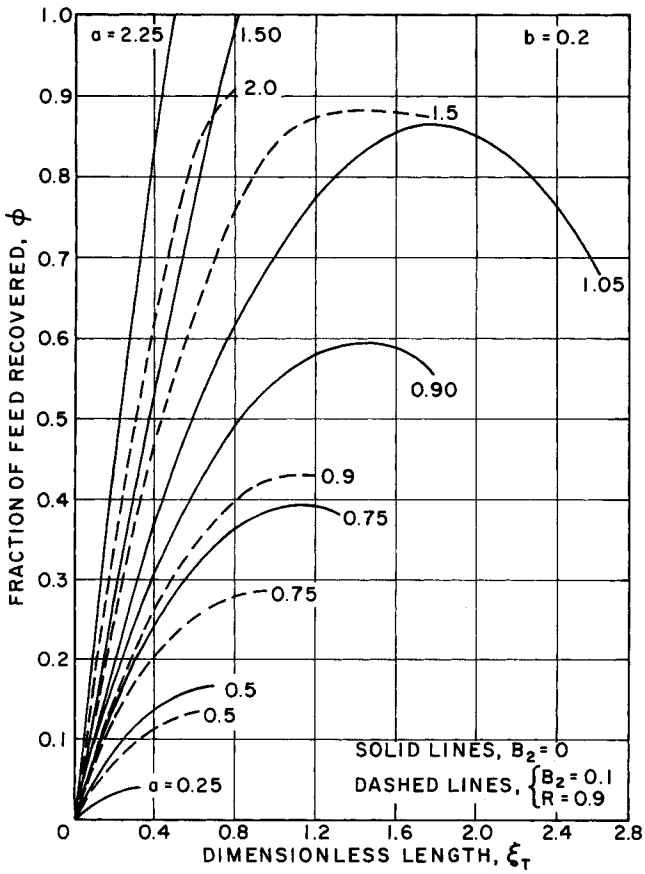

Fig. 2. Fraction of feed removed Φ vs. dimensionless length parameter ξ_T for countercurrent flow, $b = 0.2$.

Comparison of Countercurrent and Concurrent Systems, $B_2 = 0$

For small a and b, countercurrent systems are only marginally better than concurrent ones. However, as b is increased keeping a small, that is, less than unity, countercurrent units perform significantly better. At large a, the effect of b is almost negligible and the countercurrent system again is only marginally better than the concurrent system.

Numerical Solutions of Equations (34) and (36) for Concentrated Systems, $B_2 \neq 0$

Figures 2 through 6 present some results of the numerical solution of Equations (34) and (36) for concentrated systems. Note that the asymptotic value of Φ depends strongly on the parameters a and b. Larger values of both a and b yield larger fractions of feed recovered. However, the dependence of Φ on a is stronger than on b, as it is when $B_2 = 0$.

The dimensionless length parameter ξ_T required to obtain a given value of Φ depends on a, b, B_2, and R. Obviously, with larger a and b one requires less length and with larger B_2 and R one requires more system length to remove a desired fraction of feed. The effect of B_2 and b is greatest when a is small. Also, the effect of having $B_2 \neq 0$ is most detrimental to length requirements when $R = 1$.

Larger values of R imply purer product and a larger axial concentration build-up on the shell side. Since increased concentration is accompanied by increased osmotic pressure, the system productivity decreases as R increases.

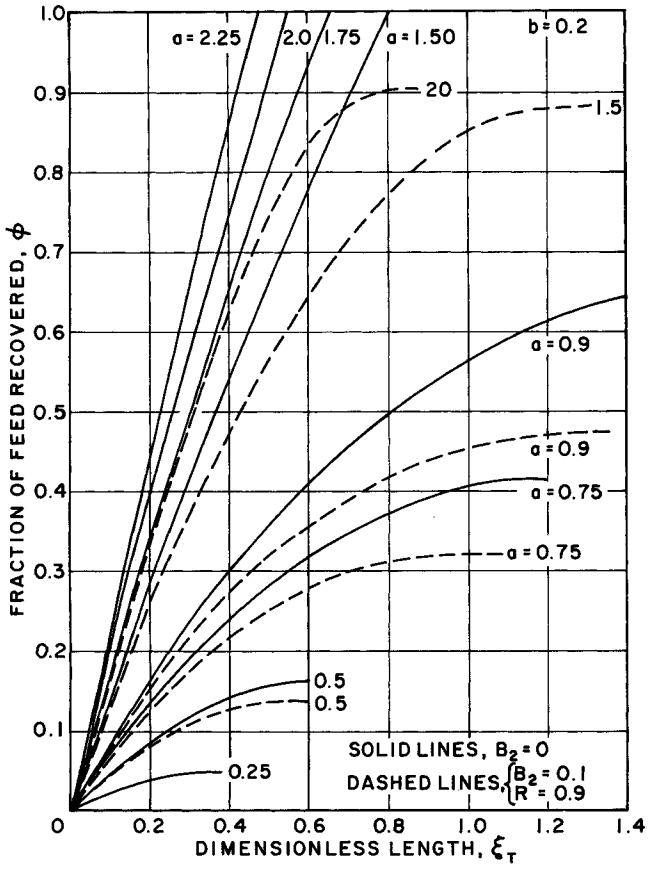

Fig. 4. Fraction of feed removed Φ vs. dimensionless length parameter ξ_T for concurrent flow, $b = 0.2$.

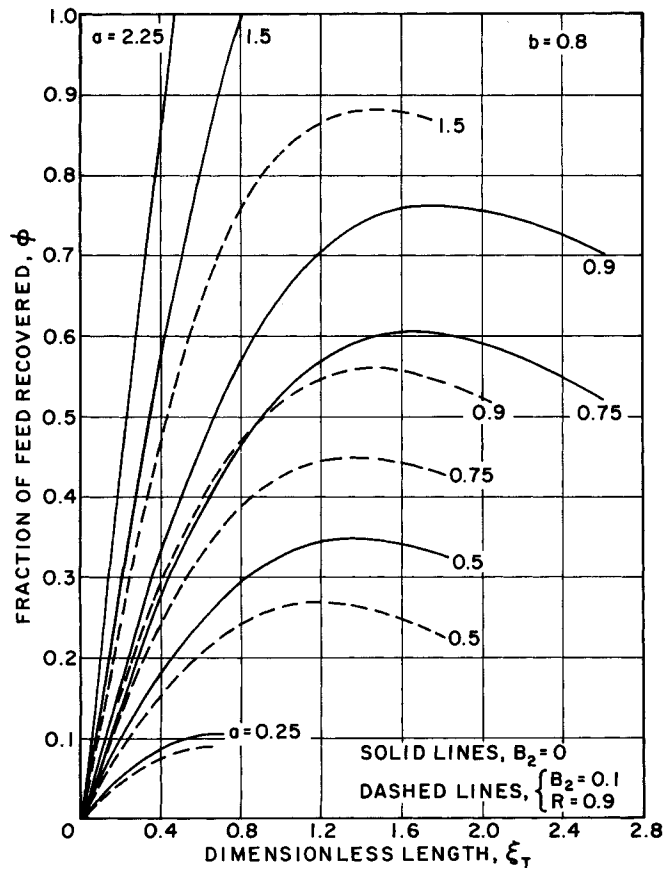

Fig. 5. Fraction of feed removed Φ vs. dimensionless length parameter ξ_T for concurrent flow $b = 0.8$.

Effect of Feed Concentration

As the feed concentration increases so does its osmotic pressure and therefore B_2 increases for a given hydrostatic feed pressure. The effect of this increase in the osmotic pressure is illustrated in Figure 7 for both countercurrent and concurrent systems. The conditions were chosen so that a comparison could be made with Cooke's data (1969). Also included in Figure 7 is the effect of increasing a which, for a given piece of apparatus and feed viscosity, corresponds to changing $\Delta P/F$. Clearly, increasing the feed pressure or decreasing the feed flow rate has a much more profound effect on productivity than does changing the feed composition by a corresponding factor.

Use of a Rejection Coefficient to Characterize Membrane Selectivity

The most extensive data reported by Cooke were the results for product concentration versus fraction of feed removed. These data enable us to examine the utility of the concept of a rejection coefficient R to characterize the selectivity of the fibers. That is, if R is reasonably constant over a sufficiently broad range of values of Φ, then the notion of a rejection coefficient is useful.

From Cooke's data (1969), Equation (43) yields the results in Table 1.

R remains constant within 2% up to 50% feed removal and varies only by about 6% up to $\Phi = 0.7$. Thus, it seems that the use of a constant rejection coefficient is

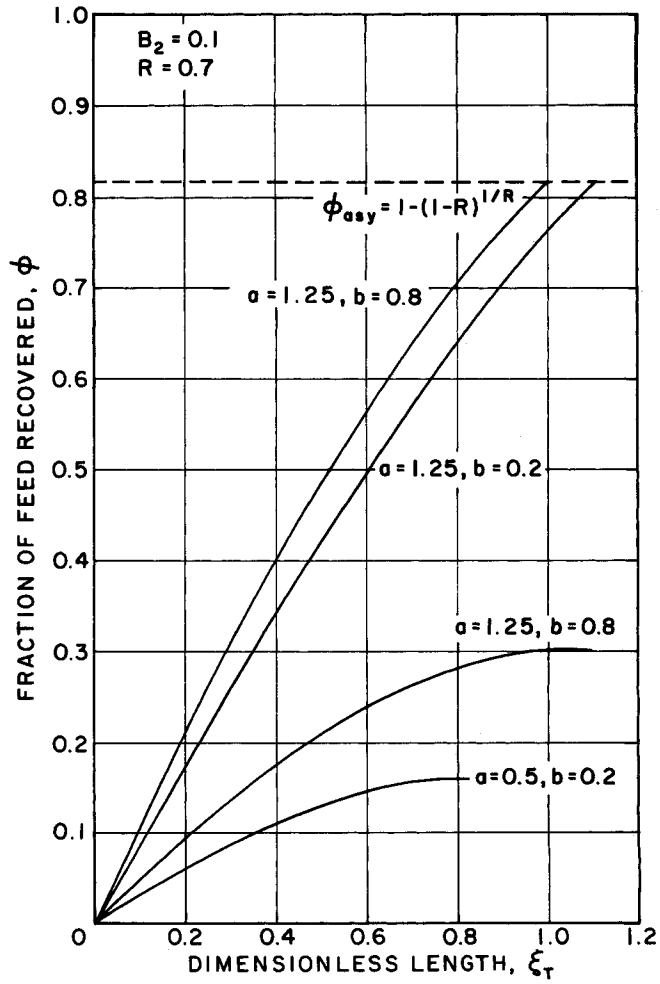

Fig. 6. Fraction of feed removed Φ vs. dimensionless length parameter ξ_T for countercurrent flow.

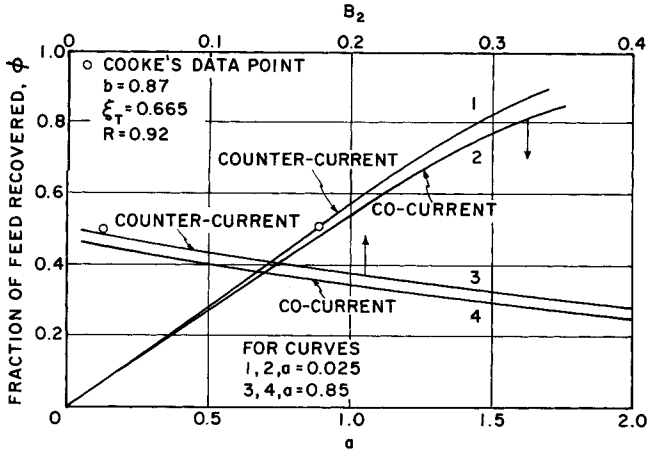

Fig. 7. Fraction of feed removed Φ vs. dimensionless parameters a and B_2 for Cooke's (1969) conditions.

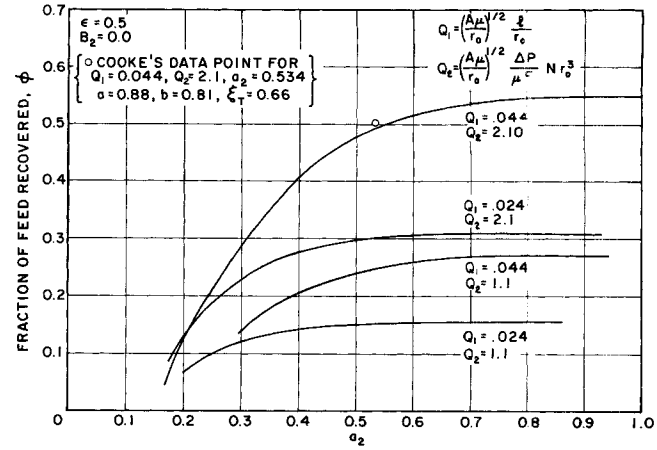

Fig. 8. Fraction of feed removed Φ vs. the inside to the outside radius ratio.

TABLE 1. REJECTION COEFFICIENT AS A FUNCTION OF Φ FROM COOKE'S DATA

Φ	c_p/c_o	R
0	0.08	0.92
0.3	0.09	0.92
0.5	0.12	0.90
0.7	0.18	0.86
0.9	0.45	0.78

reasonable. It should be noted, however, that the predicted value of c_p/c_o as a function of Φ is very sensitive to R at larger values of Φ.

Equation (43) demonstrates another important consideration; that is, with any real membrane, such that $R < 1$, an increase in system productivity is invariably accompanied by an increase in overall product concentration c_p.

Design Considerations

From the viewpoint of system design, one wishes to know how system productivity will vary as a function of the geometric factors over which the design engineer has control. That is, how do the outside radius r_o, the radius ratio $a_2 = r_i/r_o$, the void fraction ϵ, the number of fibers N, and the fiber length l affect system performance? Do optimum values exist for these parameters? Is the productivity of the system sensitive to the values of these parameters? Since we have established that countercurrent is superior to concurrent operation, only countercurrent systems will be considered in answering these questions.

Equation (44) is a remarkably simple result which can be used to obtain considerable information regarding system design. Let us consider the relationship between Φ and a_2. Equations (38a) to (38g) show that to study the effect of changing a_2 we must fix ϵ,

$$\left(\frac{A\mu}{r_o}\right)^{1/2}\frac{l}{r_o} \quad \text{and} \quad \left(\frac{A\mu}{r_o}\right)^{1/2}\frac{2\pi\Delta P N r_o^3}{\mu F}.$$

Typical results of doing this are shown in Figure 8. The values of $a = 0.88$, $b = 0.87$, $\epsilon = 0.5$ correspond with Cooke's conditions for $\Phi = 0.5$; the value of $B_2 = 0$ was chosen because it is simple and quite close to the $B_2 = 0.025$ in Cooke's experiment. Figure 8 is convenient to demonstrate the effects of the membrane constant A, the length of the system l, the feed pressure ΔP, the feed flow rate F, and the effect of decreasing the fiber wall thickness $r_o - r_i$ which corresponds to increasing a_2. It is seen that the value of a_2 at which the maximum fraction of feed is removed varies with the operating conditions and the membrane parameter A. When l/r_o and $\Delta PN/F$ are smaller, Φ_{max} is attained at smaller a_2 which implies smaller inside fiber radii r_i and thicker fiber walls. The operating conditions reported by Cooke for $\Phi = 0.5$ correspond to $Q_1 = 0.044$ and $Q_2 = 2.1$. Clearly, this result and our predictions are in good agreement; note however that an increase in Φ of 10% could be obtained with thinner walled fibers in this case. Note also that the productivity falls off rapidly under the conditions used by Cooke as wall thickness increases. Increasing the ratio of the feed pressure to feed flow rate increases system performance more than an increase in system length does.

A question of central importance is how one chooses l, N, r_o, and ϵ to maximize productivity. To do this it is appropriate to hold the fiber surface area and the system volume constant. Thus, if one chooses either ϵ or r_o the other is fixed by Equation (38a); the choice of either N or l fixes the other by Equation (38b).

To determine the proper values of these design parameters, we use Equation (44). The results for an apparatus with the surface area and volume reported by Cooke are shown in Figures 9 and 10. The theory predicts that the improvement in Φ gained by increasing the number of fibers diminishes as N gets large. For example, with $\epsilon = 0.5$, Φ increases from 0.45 to 0.52 when N increases from 20 to 30 million; however, increasing N to 40 million only increases Φ to 0.555.

Figure 10 shows that the fraction of feed removed is much less sensitive to r_o or ϵ when shorter length fibers are used because this implies lower pressure drops throughout the system. It also shows that the value of $r_o = 22.5$ microns for $l = 198$ cm, which was used for Cooke's experiments, is quite close to the best predicted value for his operating conditions. If the operating conditions are changed, say by changing the feed flow rate or pressure, the best value of r_o or ϵ will shift. However, Equation (44) can be used to carry out an optimization study of the best values of the geometrical parameters for a given range of operating conditions. To maximize Φ one would use a very short system length to reduce the pressure drop. However, with short systems, a greater fraction of the fiber area is wasted in making the end seals.

ACKNOWLEDGMENT

This work was supported in part by a grant from the Office of Saline Water, and by NSF Grant KO 34380.

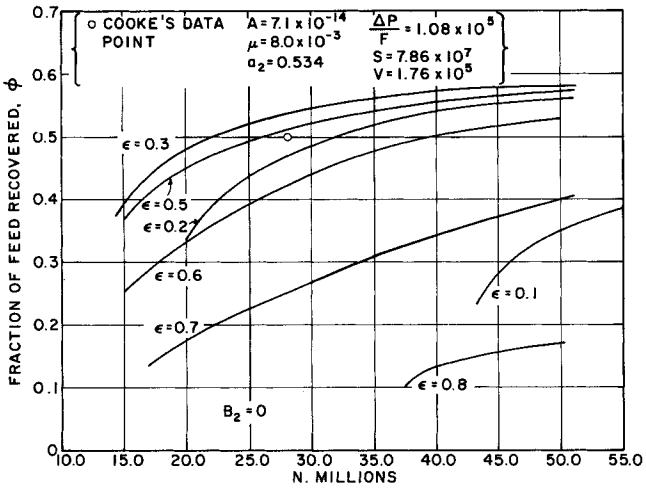

Fig. 9. Fraction of feed removed Φ vs. number of fibers N at constant $A, \mu, a_2, \frac{\Delta P}{F}, S$, and V. $B_2 = 0$.

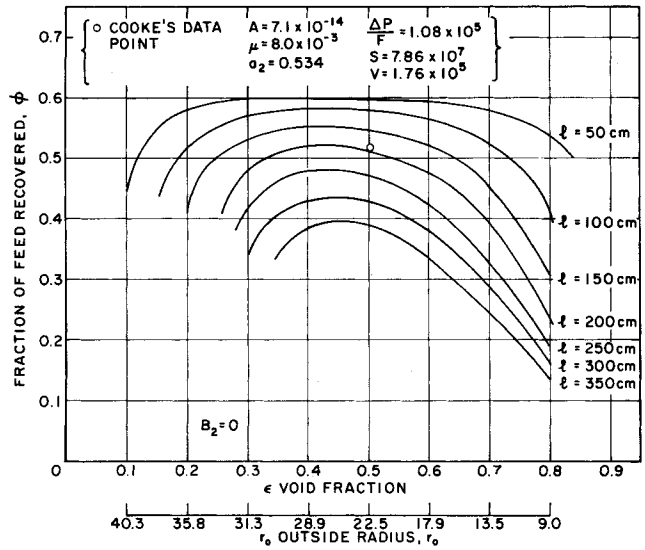

Fig. 10. Fraction of feed removed Φ vs. the void fraction ϵ and the outside radius r_0 at constant $A, \mu, a_2, \frac{\Delta P}{F}, S$, and V.

NOTATION

a = defined by Equation (33b) or (38e)
a_2 = r_i/r_o
A = membrane constant, cm² sec/g
b = defined by Equation (33c) or (38f)
B_2 = $\pi_o/\Delta P$
c_i = concentration on phase i, g mole/cm³
c_o = inlet concentration, g mole/cm³
D = diffusivity, cm²/sec
f_i = defined by Equations (14), (24) and (25)
F = feed rate, cm³/sec
g = $\dfrac{-16(1-\epsilon)^2}{2\epsilon + \epsilon^2 + 2\ln(1-\epsilon)}$
h = defined by Equation (10)
l = length of fiber, cm
N = number of fibers
p_i = pressure in phase i, g/cm sec²
P_e = $u_{1m}(0) r_o/D$, Peclet number
P_{ew} = $A\Delta P r_o/D$, wall Peclet number
ΔP = $p_1(0) - p_{atm}$, g/cm sec²
Q_1 = $\left(\dfrac{A\mu}{r_o}\right)^{1/2} \dfrac{l}{r_o}$
Q_2 = $\left(\dfrac{A\mu}{r_o}\right)^{1/2} \dfrac{\Delta P}{\mu F} N r_o^3$
r = radial coordinate
r_i = inside radius, cm
r_o = outside radius, cm
r_e = equivalent radius, cm
R = rejection parameter, defined by Equation (9)
Re = $u_{1m}(0)\, r_o/\nu$
Re_w = $A\Delta P\, r_o/\nu$
S = total surface area of all fibers, cm²
u_i = axial velocity in phase i, cm/sec
U_i = $u_i/u_{1m}(0)$
v_i = radial velocity in phase i, cm/sec
V = volume of shell, cm³
z = axial coordinate

Greek Letters

α_1, α_2 = constants defined by Equations (10a) and (18) respectively
ϵ = porosity, $(r_e^2 - r_o^2)/r_e^2$
μ = viscosity, gm/cm sec
ρ = density, gm/cm³
ν = kinematic viscosity cm²/sec
ψ_i = dimensional stream function defined by Equations (12), (13), (24) and (25)
Φ = dimensionless productivity, $[u_{1m}(0) - u_{1m}(l)]/u_{1m}(0)$
ξ = defined by Equation (33a)
π_o = feed osmotic pressure

Subscripts and Superscript

b = bulk mean
e = equivalent
i = $i = 1, 2, 3$ denotes phase (see figure 1)
o = inlet condition
m = area averaged
p = product
w = wall condition
T = total length
0 = zeroth order approximation
$'$ = differentiation with respect to r

LITERATURE CITED

Berman, A. S., "Laminar Flow in Channels with Porous Walls," *J. Appl. Phys.*, **24**, 1232 (1953).

Cooke, W. P., "Hollow Fiber Permeation in Industrial Waste Stream Separations," *Desalination*, **7**, 31 (1969/70).

Gill, W. N., L. J. Derzansky, and M. R. Doshi, "Convective Diffusion in Laminar and Turbulent Hyperfiltration (Reverse Osmosis) Systems," in *Surface and Colloid Science, IV*, Wiley, New York (1971).

Happel, J., "Viscous Flow Relative to Array of Cylinders," *AIChE J.*, **5**, 175 (1959).

Mahon, H. I., "Permeability Separatory Apparatus and Process Utilizing Hollow Fibers," U.S. 3, 228, 877 (1966).

Orofino, T. A., "Development of Hollow Filament Technology for Reverse Osmosis Desalination Systems," OSW RD 549 (1969).

Sparrow, E. M., A. L. Loeffler, and H. A. Hubbard, "Heat Transfer to Longitudal Laminar Flow between Cylinders," *ASME J. Heat Transfer*, 415 (1961).

Sparrow, E. M., and A. L. Loeffler, "Longitudal Laminar Flow between Cylinders Arranged in Regular Array," *AIChE J.*, **5**, 325 (1959).

Manuscript received December 15, 1972; revision received March 21 and accepted April 5, 1973.